

TOPICAL REVIEW

Intrinsic Josephson junctions: recent developments

A A Yurgens

Department of Microelectronics and Nanoscience, Chalmers University of Technology, S41296 Gothenburg, Sweden

Received 12 October 1999, in final form 2 May 2000

Abstract. Some recent developments in the fabrication of intrinsic Josephson junctions (IJJ) and their application for studying high-temperature superconductors are discussed. The major advantages of IJJ and unsolved problems are outlined. The feasibility of three-terminal devices based on the stacked IJJ is briefly evaluated.

1. Introduction

More than a decade has passed since the discovery of high-temperature superconductivity (HTS), but it still remains a challenge for physicists to derive a model which would explain the main experimental features of the new superconductors. In the majority of theoretical models of HTS, it is assumed that the normal and superconducting state properties of the layered high- T_c cuprates derive mainly from the properties of the CuO_2 planes, while the other structural components in the unit cell act simply as charge reservoirs. The interlayer coupling has largely been considered as the mechanism of controlling the carrier concentration in the CuO_2 planes.

The c -axis (or out-of-plane) coupling has become especially important since the interlayer tunnelling model of HTS has been developed [1]. In this model, the energy gain that drives the formation of Cooper pairs is associated with a decrease of the kinetic energy due to the easy motion of the pairs accompanied by the impeded single-particle tunnelling along the c -axis.

Another important question is whether the normal state out-of-plane transport is coherent or not, and what the origin of the ‘semiconducting’ c -axis resistivity in the cuprates is. Theories of out-of-plane transport differ in whether the zero-temperature state of cuprates is ‘metallic’ with a finite c -axis resistivity ρ_c , or insulating with an infinitely large $\rho_c(T \rightarrow 0)$. Major c -axis transport models have been examined in the review article by Cooper and Gray [2].

The physics of vortices has become one of the most quickly developing areas of modern physics. HTSs with their large anisotropy and thermal fluctuations represent a large research field where it has become possible to observe many new effects experimentally. A clear experimental evidence for melting of the classic Abrikosov vortex lattice in a wide temperature range below the superconducting critical temperature T_c [3] has verified a number of theories and stimulated further experimental and theoretical studies.

The intrinsic Josephson effect (IJE) as a tunnelling of the Cooper pairs between adjacent CuO_2 planes inside the highly anisotropic layered HTS is an integral part of many theories on this subject and is of primary importance for deriving properties of the vortex system [4]. It was experimentally confirmed by Kleiner and co-workers that the intrinsic tunnelling of the Cooper pairs indeed takes place in $\text{Bi}_2\text{Sr}_2\text{CaCu}_2\text{O}_{8+\delta}$ (Bi-2212) [5] and other anisotropic single crystals ($\text{Tl}_2\text{Sr}_2\text{Ca}_2\text{Cu}_3\text{O}_{10+\delta}$ (Tl-2223) and $(\text{Pb}_y\text{Bi}_{1-y})_2\text{Sr}_2\text{CaCu}_2\text{O}_{8+\delta}$ (Bi(Pb)-2212)) [6]. In these experiments both dc and ac Josephson effects have been observed. The current–voltage (I – V) characteristics for current flow in the c -axis direction exhibited large hysteresis and multiple branches. These results clearly showed that all the materials behave like stacks of superconductor–insulator–superconductor (SIS) Josephson junctions, see figure 1. The experimental discovery of IJE in HTSs is very important because it sets in the limitations on possible theories of HTS and requires reassessment of many works. The experimental works involving c -axis tunnelling in highly anisotropic HTS but failing to demonstrate IJE should be regarded with discretion.

A review of all these observations and the present status of research regarding theoretical understanding of the intrinsic Josephson effect has been given some time ago [7, 8]. For an unsorted collection of recent works on the intrinsic Josephson effect, see [9]. In this article, I will try to demonstrate that the intrinsic tunnelling is not only an interesting subject for research by itself, but has already become a powerful *tool* for studying the nature of HTS and physics of vortices, and is on its way towards applications in superconducting electronics.

The article is organized in the following way. First, I will overview existing experimental techniques for making the intrinsic Josephson effect observable in transport measurements. Then, a discussion of the particular I – V characteristics will be given with emphasis on the superconducting gap and sub-gap features as seen from the

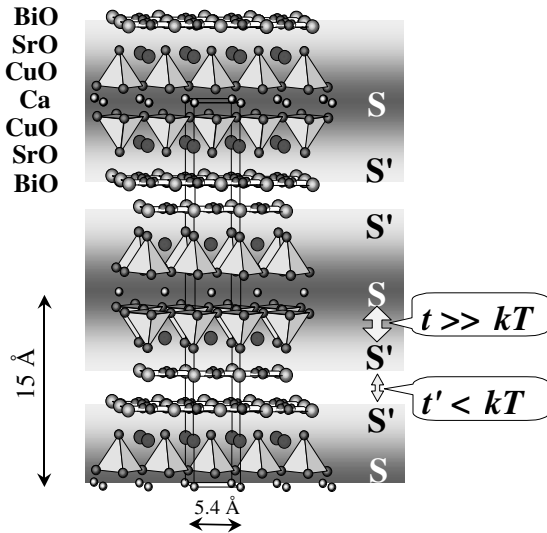


Figure 1. The crystal structure of Bi-2212. The darkened regions represent the possible variations of the superconducting energy gap parameter.

intrinsic Josephson tunnelling. The heating problem will be discussed. The effect of temperature, magnetic field and pressure on the c -axis critical current and form of the I - V characteristics and also implications for some theories of HTS will be described. In conclusion, three possible configurations of devices will be evaluated.

2. Experimental techniques

2.1. Single crystals. ‘As is’

To see the IJE from the transport measurements one can simply apply the current in the c -axis direction of a single crystal and monitor the voltage [5]. However, since common single crystals are $\sim 1 \text{ mm}^2$ in size in the lateral direction, and the c -axis critical current density j_c is of the order of 10^3 A cm^{-2} [5, 6], the c -axis critical current I_c can be as high as 10 A. Given the contact resistance of 0.1Ω , the Joule heating of $\sim 1 \text{ W}$ should be acknowledged. This means that one should use tiny crystals $\lesssim 0.1 \times 0.1 \text{ mm}^2$ in size [5, 6] to be able to reach the critical current without heating problems and have some dexterity for handling such specimens.

Annealing at high temperature ($>450 \text{ C}$) can be used to obtain good contacts. The annealing however inevitably leads to the diffusion of metal in the c direction and along any micro-cracks near the surface [10], which affects the genuine interlayer characteristics[†]. Moreover, any high-temperature processing will result in the diffusion of oxygen in or out of the sample, so that the level of doping may become undetermined.

The I - V characteristics of even small bulk crystals with good contacts can still be affected by Joule heating due to the relatively large thickness of single crystals. A common thickness of Bi-2212 single crystals is about $3\text{--}10 \mu\text{m}$, which

[†] The diffusion coefficient D of Ag in the c -axis direction of a Bi-2212 single crystal is $\approx 2.7 \times 10^{-14} \text{ cm}^2 \text{ s}^{-1}$ at 650°C [10]. After $t = 1 \text{ h}$ of annealing at this temperature, Ag will diffuse as deep as $\Lambda \sim \sqrt{Dt} \sim 10^{-5} \text{ cm}$, i.e. affecting ~ 100 surface IJJ.

means that there are usually about $N \sim 10^3\text{--}10^4$ intrinsic Josephson junctions (IJJ) in series across such a thickness. Assuming that each junction has a characteristic gap voltage equal to the superconducting energy gap 2Δ ($\sim 25\text{--}50 \text{ meV}$), we obtain the sum-gap voltage to be $\sim 2N\Delta \sim 10\text{--}200 \text{ V}$. We see again that the heating is a persistent problem for single crystals of usual size.

2.2. Lithography. ‘Trimming’ and ‘carving’

An alternative approach to decrease the heating and facilitate study of an individual tunnel junction is to decrease the number of active junctions in the c -axis direction and to decrease their area by using existing and well developed photolithography and chemical or Ar-ion milling techniques for etching small mesa-structures on the surfaces of single crystals or thin films [11–25]. Using such technologies one can make areas as small as $2 \times 2 \mu\text{m}$ [22], and heights down to $\sim 15 \text{ \AA}$ [13, 26], which in fact corresponds to the thickness of one IJJ in Bi-2212.

The technologies of mesa fabrication can differ in detail, but the general features remain the same, and are sketched in figure 2.

- The single crystal is first glued on the substrate by an epoxy. This step is obviously absent in the case of a thin film.
- Then, in order to get a fresh surface, the single crystal is cleaved with the aid of adhesive tape. Also absent for the thin film.
- To protect the surface from water and chemicals during the photolithography, a thin layer of gold or silver is deposited immediately after the cleavage.
- Photolithography is used to pattern the photoresist and define small mask structures on the surface.
- Ar-ion or chemical etching is applied for some calibrated time to etch down unprotected by the photoresist parts of the single crystal or thin film.

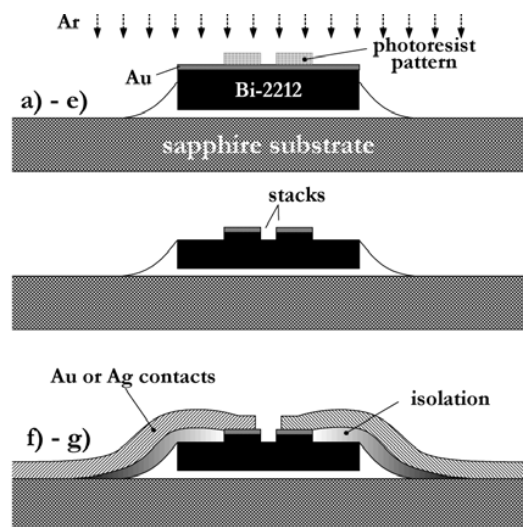


Figure 2. Fabrication process for making stacks of intrinsic Josephson junctions. See the text for explanations.

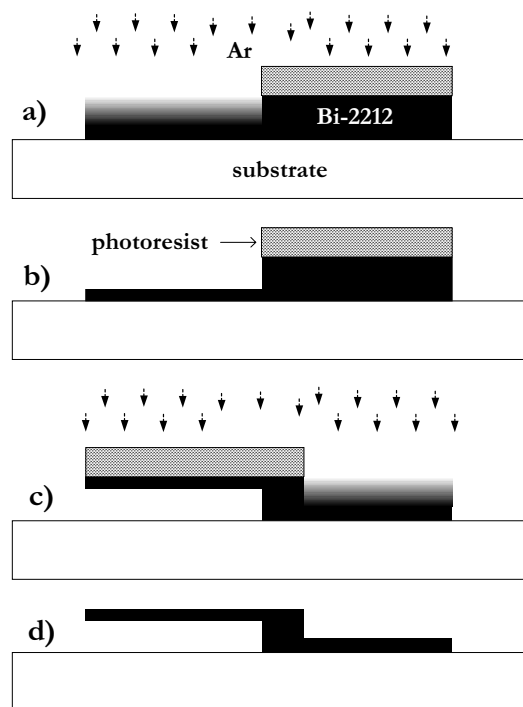


Figure 3. Schematic view of the stack fabrication from a Bi-2212 whisker.

- (f) A layer of insulation is applied and patterned accordingly (self-alignment and lift-off techniques may be used in the case of thin films which have a flat and smooth surface across the whole chip, while in the case of single crystals glued on a substrate this is hard to implement).
- (g) A thin film of normal metal is deposited and patterned to form contacts to the top of each mesa. In the case of small-area mesas there is only one contact on each mesa, while for larger mesas one can separate current and potential leads, which allows advantageous four-probe measurements to be performed.

Stacks of intrinsic junctions were also made from Bi-2212 whiskers [27, 28], which are known to have the best crystal structure [29] and to have small enough sizes to apply the minimum of Ar-ion etching, see figure 3. The whiskers grow in the a -direction and usually have small dimensions in both the b - and c -directions. As is seen from figure 3, there are only two steps of Ar-ion milling in the process of making stacks. An obvious advantage of this geometry is the absence of normal metal contacts in the vicinity of the stack, which can provoke non-equilibrium quasiparticle injection effects at high bias currents.

Recently, very small submicrometre-sized stacks have been fabricated using the focused-ion-beam (FIB) technique [30, 31]. The authors claimed to substantially reduce the effects of self-heating and quasiparticle injection, and avoid the ‘back-bending’ of I - V characteristics at the gap voltage in their submicron stacks [31].

2.3. Vicinal thin films

One can also use high-index substrates which are cut at a small angle to one of the main directions for making stacked

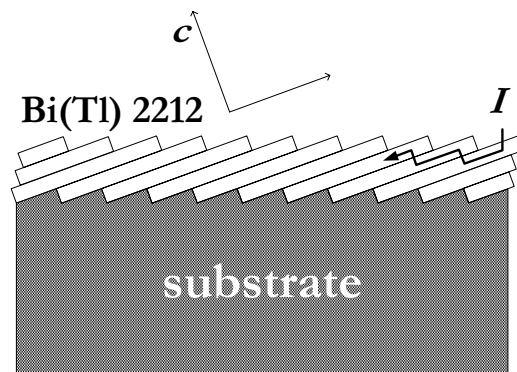


Figure 4. Schematic view of vicinal Bi- or Tl-2212 thin film. Note that the current flows in both ab - and c -axis directions.

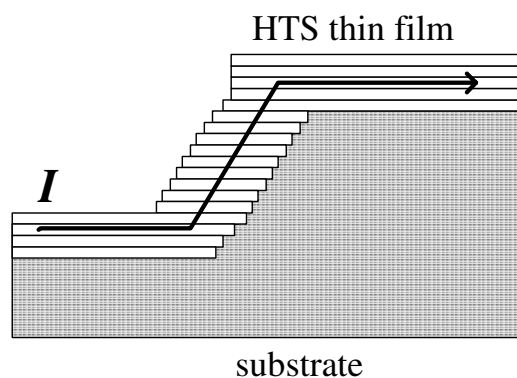


Figure 5. Schematic view of step-edge Bi- or Tl-2212 intrinsic junctions. The height of the step and the thickness of the thin film dictate the resulting number of junctions in series.

IJJ. The epitaxial thin film grows in the same vicinal direction on such a substrate, which means that the film is made of many closely spaced ‘steps’, see figure 4. The current then flows along both the ab -plane and the c -axis directions. This geometry is advantageous for applications, and facilitates the heat escape from the stack into the substrate [32, 33, 34]. Step-edges etched into the single-crystalline substrates can also be used for the fabrication of stacked IJJ [35]. Deposition of Bi-2212 or Tl-2212 thin films on such a substrate results in a geometry very similar to the stacks made from Bi-2212 whiskers, see figure 5 [35]. The height of the step and the thickness of the thin film dictate the resulting number of intrinsic junctions in series.

One more way to isolate the intrinsic junctions is to employ different orientations of grains in a polycrystalline Bi-2212 thin film. While a large part of the thin film is generally c -axis oriented, there are sometimes several needle-like grains of a ‘wrong’ orientation ((110) instead of (001)) grown in the body of the thin film. In such a grain, the c axis lies parallel to the substrate surface. By forming a bridge across the grain one can get a weak link consisting of many IJJ [36]. However, the critical current density of such junctions was found to be very low, about 30 A cm^{-2} , which probably demonstrates poor quality of the grain [36].

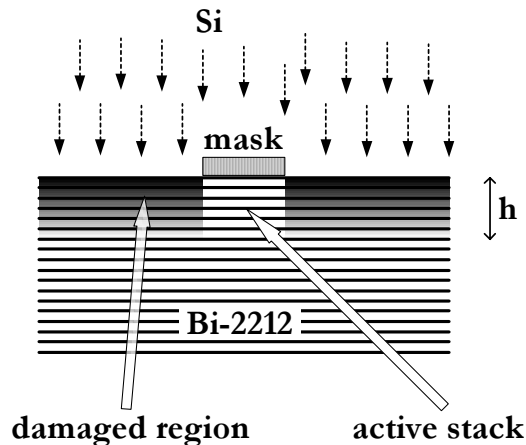


Figure 6. Schematic view of superconducting stack of Bi2212 IJJ imbedded in the bulk crystal. The active stack height h is determined by the Si-ion penetration depth.

2.4. Ion implantation and artificial multilayers

Nakajima *et al* [37] have recently fabricated superconducting stacks of Bi-2212 IJJ imbedded in a non-superconducting matrix of the same material where the superconductivity has been destroyed by the Si-ion implantation. The height of the active stack is approximately set by the depth of Si implantation, see figure 6. Such stacks may have some advantages. For instance, no isolation layer between the main part of the crystal and the leads to the top of the stack may be needed because a high concentration of implanted atoms can possibly make the surface layer of Bi-2212 completely non-conducting, facilitating wiring to the stack. Furthermore, the self-alignment technique may be used to fabricate sub-micron-sized stacks of IJJ.

A layer-by-layer all-MBE technique for growth of high-temperature superlattices allows one to go beyond normal stoichiometric chemical composition of the thin film and engineer a specified artificial compound [38]. Josephson junctions fabricated from such multilayers may also have SIS-type current–voltage characteristics which is obviously very important for technical applications [38].

3. c -axis current–voltage characteristics

Typical I – V characteristics for the stack with 130 IJJ are shown in figure 7(a) for small voltages. I – V s of an artificial three-junction Nb/Al–AlO_x/Nb stack are presented in figure 7(b) for comparison. The two sets of characteristics are quite similar. The I – V characteristics of one-dimensional (1D) arrays of Josephson tunnel junctions consist of several branches, each corresponding to one, two, three, etc individual junctions switching to quasiparticle state as the bias current exceeds the corresponding critical current. If the critical currents of all the junctions in the stack have close values, the switching from the zero-voltage state may not necessarily happen to the closest branch. The system can ‘jump’ over several branches. Such an event is often taken as a signature of the phase locking of several junctions in the stack. Then, these junctions effectively act as a single one with a larger gap voltage.

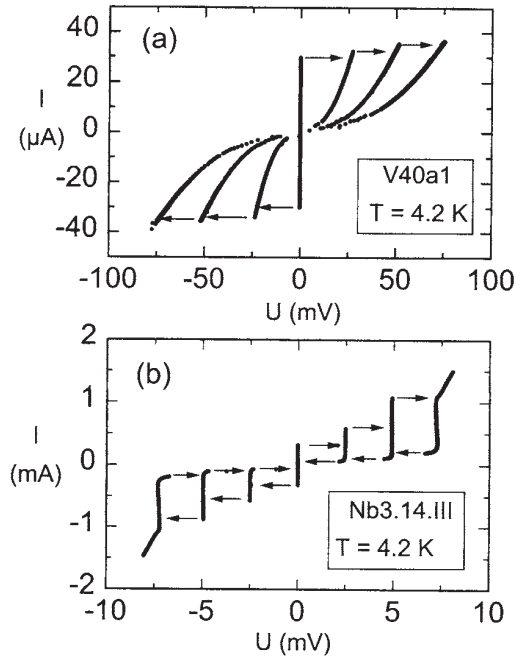


Figure 7. (a) First three branches of the I – V characteristic of a $\text{Tl}_2\text{Ba}_2\text{Ca}_2\text{Cu}_3\text{O}_{10+\delta}$ step stack with a total number of 130 junctions; (b) I – V characteristics of an artificial three-junction Nb/Al–AlO_x/Nb stack. Arrows indicate voltage switching. (From K Schlenga *et al* 1998 *Phys. Rev. B* **57** 14 518 [57]; ©1998 The American Physical Society.)

In order to trace a specified quasiparticle branch, one has to decrease the bias current immediately after the system happened to switch to a desired branch. If the system ‘missed’ it, one has to return to the zero-voltage state and make a new attempt. Note that there is no one-to-one correspondence between branches and particular junctions in the stack. One and the same branch of the I – V characteristic may result in concurrent action of different junctions in the stack at different instances.

3.1. Superconducting energy gap

The quasiparticle branches in figure 7(b) are separated in voltage by ~ 2.5 mV, which corresponds to twice the superconducting energy gap Δ_{Nb} for Nb, $2\Delta_{\text{Nb}}/e$, in accordance with S–I–S character of each junction. Furthermore, the branches are almost vertical at these voltages. The corresponding jumps in Bi-2212 are about 25 mV, and the current rise is gradual for all branches. Assuming that the same relation holds for the voltage jumps, $\delta V \approx 2\Delta/e$, we obtain that $\Delta \sim 12$ – 13 meV for tunnelling in the c -axis direction. This value is about one half of the value obtained from the scanning tunnelling microscopy (STM) data [39], or break-junction technique [40].

Absence of the normal-state parts of I – V characteristics in figure 7(a) does not allow the exact detection of the superconducting-gap singularity, although in some experiments it was observed that the first branch had indeed almost vertical current rise at ~ 25 mV [26].

Several explanations have been suggested. The trivial heating explanation implies that the mesa can be up to several

tens of Kelvin warmer than ambient temperature due to power dissipation in the junctions and low thermal conductivity of the material. The small Δ is then simply due to decreasing with temperature $\Delta(T)$. On the other hand, the more IJJ switch to the normal state, the more power is dissipated. Therefore the voltage jumps should decrease for branches with higher count numbers. This is not the case in experiment with $N < 15\text{--}20$.

Non-equilibrium quasiparticle self-injection, which is typical for stacks of tunnel junctions, can also cause the gap to decrease [41]. Since the thickness of each electrode of an individual IJJ is about 3 Å only, the quasiparticles generated in one junction can easily penetrate others and increase the quasiparticle population. Furthermore, a charge imbalance at high current can initiate an additional voltage between potential and current leads and cause the ‘back-bending’ often seen in the four-probe and less commonly, in three-probe measurements. At low currents, the results of three- and four-probe measurements are basically similar, and the separation in voltage between the branches is the same—20–30 meV [25, 35, 42, 43, 44, 45].

The proximity effects suggested in [26] could explain both the reduced value of the gap parameter and its strong temperature dependence. Assuming that the BiO layers can be metallic or even superconducting due to proximity effects, the actual schematics of the IJJ becomes SS’–I–S’S rather than S–I–S. Then, the intrinsic tunnelling shows a smaller gap voltage corresponding to a weaker superconductivity (S') of the BiO layers, $\delta V = 2\Delta_{S'}$, see figure 1 [26]. The reduced and strongly temperature dependent energy gap has also been observed in some angle-resolved-photoemission (ARPES) experiments [46].

In their *three*-probe measurements on small mesas, Itoh *et al* [16] managed to reach the normal-state parts of the tunnelling I – V characteristics with no negative dynamic resistance†. To reduce the electrical resistance of contacts to the mesas, they were annealed at 650 °C. The authors reported $\Delta \sim 25$ meV, which is in accordance with STM or break-junction experiments.

Generally speaking, the identification of tunnel-spectra peaks for HTS does not seem to be an easy task, because the density of states $\nu(E)$ of a system composed of several 2D layers with different electron-coupling constant has quite a complicated structure. The maximum in $\nu(E)$ thus does not necessarily correspond to the order-parameter value [47].

3.2. Sub-gap current

For common BCS-type superconductors, the sub-gap current I_{sg} is negligible below the gap at low temperatures, $I_{sg} \sim V/R_N \exp(-\Delta/k_B T)$. R_N is the normal state resistance of a tunnel junction, and k_B is the Boltzmann constant. For $\Delta \approx 12\text{--}13$ meV, $V \sim 1$ mV, $R_N \sim 1 \Omega$ [13] and $I \sim 10^{-17}$ A. Despite a large superconducting gap, IJJs have a non-zero quasiparticle current below the gap at all temperatures.

A non-zero I_{sg} suggests a non-zero quasiparticle density of states below the gap, which is consistent with the most

popular d-wave superconductivity-model of cuprates, when the superconducting energy gap parameter has nodes in certain directions of the k -space along the Fermi surface. However, other scenarios like resonant tunnelling [48, 49, 50] and pair-breaking effects [51] can also explain a non-zero sub-gap current.

In the simple approximation, the tunnelling current between two superconductors is [52]:

$$I(V) \propto \int_{-\infty}^{\infty} \nu(E) \nu(E - eV) \{f(E - eV) - f(E)\} dE \quad (1)$$

where $f(E)$ is the Fermi function. For the suggested d-wave superconductors the density of states $\nu(E)$ is:

$$\nu(E) = \frac{1}{2\pi} \int_0^{2\pi} \text{Re} \left(\frac{E d\theta}{\sqrt{E^2 - \Delta_0^2 \cos^2(2\theta)}} \right) \quad (2)$$

where $\theta = \arctan(k_y/k_x)$ is the angle in the k -space, and Δ_0 is the maximal value of the energy gap parameter.

Numerical computation of equation (1) yields curves very similar to the experimental ones [18]. On closer examination, this similarity is, however, noted to be qualitative only. The experimental $dI/dV(V)$ -dependence always shows an upturn at high bias current, absent in the results of computing according to equation (1). This dissimilarity was somewhat reduced by taking into account the heating and non-equilibrium effects [18]. Although reproducing the main features of the experimental I – V -characteristics, including the back-bending, the quality of the final fit of experimental points to theoretical equations is not perfect, see figure 6 in [18]. The necessity of introducing more fitting parameters and working mechanisms somewhat taints the conclusion of consistency between the d-wave superconductivity and intrinsic Josephson tunnelling effect, and poses again the question on the heating and non-equilibrium effects as inherent properties of the stacked tunnel junctions, see below.

Theoretical analysis of the sub-gap current of IJJ in Bi-2212 stacks has been undertaken in [31]. The experimental data were analysed in the framework of the BCS d-wave pairing model inside the layers, taking into account both the reduced, in comparison with the Ambegaokar–Baratoff value, j_c , and the particular form of the resistive branch of the I – V characteristic. The authors conclusion was that the clean limit of the above-mentioned model with a resonant interlayer scattering and coherent tunnelling contribution provided a consistent description of the experimental data [31].

4. Other materials

The intrinsic Josephson effects in transport properties were also observed in other basic HTS materials, like YBCO and LSCO. The former material needs to be annealed in non-oxygen atmosphere or vacuum in order to substantially increase the anisotropy and observe the intrinsic Josephson tunnelling. Several reports have been published to date [53–55]. However, the resulting characteristics are far from perfect to allow the junctions to be utilized for practical applications or basic studies. These experiments demonstrate

† The S-shaped characteristics with a heavy back-bending at the gap voltage usually witness to heating or non-equilibrium effects in the stacks of tunnel junctions.

however that the intrinsic Josephson tunnelling is a common property of almost all anisotropic high- T_c compounds, which is of course important.

5. Heating and non-equilibrium effects

All high-temperature superconductors have a comparatively low thermal conductivity, which makes them prone to local overheating. Taking the thermal conductivity $\kappa \sim 10^{-2} \text{ W cm}^{-1} \text{ K}^{-1}$ [56], geometrical factor $S/L \sim 10^{-3} \text{ cm}$ (a typical area S of mesas $\sim 100 \mu\text{m}^2$ and the thickness of a single crystal $L \sim 10 \mu\text{m}$), we obtain the thermal conductance of about 10^{-5} W K^{-1} . Even very small power dissipation of 1 mW (for $I \approx 3 \text{ mA}$ and $V \approx 300 \text{ mV}$, corresponding to the sum-gap voltage of about 10 IJJ) yields the overheating $\delta T \sim 100 \text{ K}$.

The thickness of the thin films is an order of magnitude smaller than that of a single crystal. This implies that the heat sink is much better for thin films than for stacks on the surface of single crystals, and therefore the overheating in the former case should be noticeably smaller. However, looking at the published data, it is seen that the separation between the quasiparticle branches is the same, 20–30 meV [19, 57]. Furthermore, the heat release is proportional to the number of IJJ in the quasiparticle state. The larger the count number of the quasiparticle branch, the larger heat release and the smaller voltage jumps should be seen in I - V curves. This is again in contrast to experiments, where branches almost equidistant in voltage are usually observed for not too many IJJ in the stacks (< 10 –15).

Pulse measurements [58–60] can be employed to avoid the heating. The heat diffusion time τ for the above mentioned geometrical sizes can be roughly estimated taking the specific heat $c_h \sim 0.2 \text{ J kg}^{-1} \text{ K}^{-1}$ at 4.2 K [61] and the density $\rho \approx 6.5 \text{ g cm}^{-3}$: $\tau \sim c_h \rho L^2 / \kappa \approx 15 \text{ ns}$ at low temperatures. The longer diffusion times $\sim 1 \mu\text{s}$, measured in [58, 59, 60] may possibly be attributed to an annexed mass of the isolation and metal leads to the mesas.

In the pulse measurements on the stack with ≈ 50 IJJ [42], the sum-gap voltage (about 1 V) was essentially dependent on the bias-current pulse duration. However, the separation between branches lying close to the zero-voltage state did not depend on it, strongly suggesting that the heating effects are not very important in the stacks with minimal number of IJJ and at low bias current [42].

Simultaneous dc transport and the mesa-temperature measurements have recently been performed [59, 58], allowing corrections for dc heating to be made. Using the contact resistance for the temperature sensing it was possible to trace out changes of the temperature during the measurements. Significant heating of up to 25 K was observed at low temperatures.

The experiments on sub-micrometre-sized IJJ fabricated from Bi-2212 single crystalline whiskers [30, 31] are of particular interest because of a small residual critical current. The authors observed no ‘back-bending’ of their I - V characteristics, suggesting no heating problems in the super-small stacks. Simple estimations show, however, that although the heat release is indeed dramatically reduced in such stacks, the heat escape worsens also. Assuming the

same value of $\kappa \sim 10^{-2} \text{ W cm}^{-1} \text{ K}^{-1}$, and the geometrical factor $S/L = (1 \mu\text{m})^2 / 1 \mu\text{m} \approx 10^{-4} \text{ cm}$ [30, 31], we obtain the thermal conductance of the heat sink to be about 10^{-6} W K^{-1} , i.e. an order of magnitude less than in the case of mesas. The dissipation of merely 0.1 mW causes the estimated overheating to be the same, 100 K.

These estimations can easily turn wrong because they implicitly use the assumption that the heat escape from the mesa takes place via diffusion of quasiparticles into the bulk of the single crystal. This assumption is certainly invalid in the case where the mesa height h is 100–200 Å only, because the mean free path of low-frequency phonons which make an essential contribution to the heat transport at low temperatures can be $l_p \sim 1 \mu\text{m} \gg h$ [56]. Such (non-equilibrium) phonons created in one of the IJJ can shoot through the whole thickness of the mesa before releasing their energy in the bulk of the single crystal. This underlines again the need for careful theoretical description of the non-equilibrium effects in the layered superconductors.

It has always been a problem to distinguish heating and non-equilibrium effects in stacks of tunnel junctions. An attempt has recently been made to see the charge-imbalance non-equilibrium effects in the surface CuO_2 layer of a Bi2212-mesa in contact with a normal metal [62]. It has been observed that the resistance of such a contact increases several times under the action of radio-frequency irradiation, suggesting that, in fact, the non-equilibrium effects can be independently measured.

6. Experiments with intrinsic Josephson junctions

6.1. Intrinsic tunnelling spectroscopy

Tunnelling spectroscopy has traditionally been used to probe the density of electronic and phononic states [52, 63]. The high-temperature superconductors have been intensively studied by such methods ever since these superconductors were discovered [64–66].

Scanning tunnelling spectroscopy (STS) measurements are usually made in standard experimental set-ups with a sharp metal tip as a probe electrode placed near the surface of the investigated material. All these measurements probe basically the surface properties of the specimen. The surface of HTS is known to deteriorate due to atmospheric moisture, for instance. It is therefore significant to prepare a fresh surface by cleaving single crystal in high vacuum and low temperature [39]. Even then, the question about how well the surface measurements reflect the bulk properties remains open.

The intrinsic Josephson junctions offer a unique possibility of observing the corresponding quasiparticles involved in the tunnelling processes *inside* the single crystal, far away from the surface. This is an indisputable advantage of IJJ, which is however tainted by the scarce knowledge of the properties of intrinsic ‘electrodes’ and the absence of a well established model of superconductivity in the cuprates.

In the first experiments on IJJ, it was noticed that there were pronounced features not only in the $dI/dV(V)$ curves, but sometimes even in the I - V itself for $V < 2\Delta(T)$ [45], see figure 8. The position in voltage of these features did not

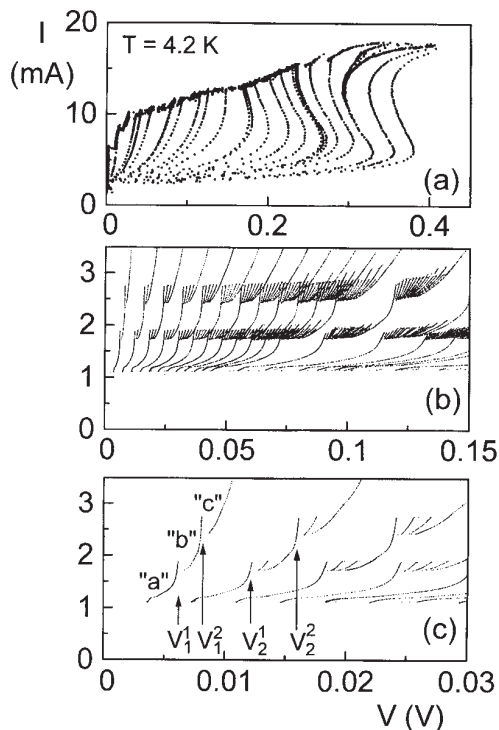


Figure 8. (a) Overall I - V characteristic of a Bi-2212 sample exhibiting multiple branching in the resistive state (not all branches are traced out for clarity). (b) The same I - V characteristic on expanded scales showing sub-gap structures at bias currents of about 1.9 and 2.7 mA. (c) Enhanced resolution of the first three branches. (From K Schlenga *et al* 1996 *Phys. Rev. Lett.* **76** 4943, [45]; ©1996 The American Physical Society.)

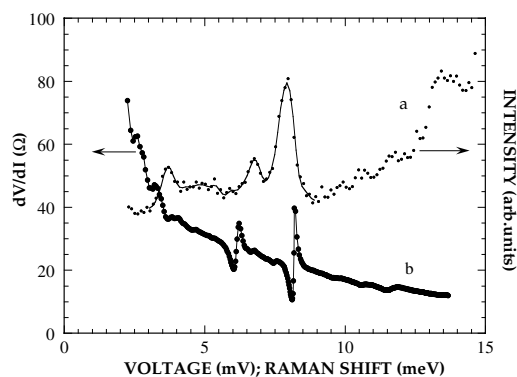


Figure 9. Comparison of tunnelling and Raman spectroscopy measurements on one and the same specimen [67].

depend on the temperature, relatively small magnetic field, and geometrical sizes of the samples [45, 67, 68].

Structures in the tunnelling spectra are usually ascribed to phononic or electronic origin (or a combination of the two) [63]. Phonon induced structures are usually weak, and are only seen in the second derivative of the measured I - V characteristic. The corresponding voltages are related to the temperature dependent superconducting gap voltage. The independence of the structure on the temperature rules out a direct phonon-assisted tunnelling mechanism [45, 67, 68].

A thick mechanism, suggested in [67] was provoked by an evident one-to-one correspondence between the intrinsic

tunnelling spectra and the Raman spectra obtained on one and the same single crystals [67], see figure 9. However, the absence of a particular theoretical model did not allow the authors to go beyond the purely speculative description that time [67].

Several explanations have since been introduced [45, 69]. One of them phenomenologically suggested a kind of rectification of the Josephson radiation in the resistively-shunted-junction (RSJ) model.

The resonant coupling mechanism between infrared-active optical c -axis phonons and oscillating Josephson currents was also proposed for explaining the sub-gap features [69]. Simple in physics, the model explained all experimental features. It is however hard to find accurate spectroscopic measurements of infrared phonons of Bi-2212 or Tl-2212 [70] in this range, which makes ultimate comparison with the theory complicated.

A similar model has recently been proposed, which incorporated all sorts of lattice excitations [71]. It was shown that the dI/dV features should exist at energies corresponding to the Raman peaks as well. The authors make reference to the break-junction experiments by Ponomarev *et al* [72], where many features were observed in the dI/dV curves, which were ascribed to Raman-active phononic excitations. The problem of the sub-gap structures in the tunnelling spectra of high- T_c materials does not therefore appear to be ultimately solved. More independent high-resolution Raman and low-energy infrared spectra are needed to derive the right model.

6.2. Pseudogap

The pseudogap (PG) in the single-particle excitation spectra is one of the indications on the unusual pairing mechanism in high- T_c superconductors. This phenomenon has attracted much attention in recent years, both experimentally [73, 74] and theoretically [74, 75]. Signatures of pseudogap in the normal state of quasiparticle excitation spectra have been seen in various experiments, like STM, NMR, specific heat, optical measurements, etc.

Common to all tunnelling experiments are I - V nonlinearities at temperatures well above T_c , corresponding to increasing c -axis resistivity on decreasing temperature. Several studies involving intrinsic tunnelling have been also performed [76–83]. However, intrinsic tunnelling experiments can have a problem of internal overheating at the large bias current needed to reach the normal-state parts of the tunnelling curves, see section 5. An attempt to overcome the heating problem has been made in the work by Suzuki *et al* [77]. The authors used short-pulse measurements and very thin stacks containing $N \sim 10$ IJJ to avoid the heating problems in their measurements on slightly overdoped samples of Bi-2212 single crystals.

The typical $dI/dV(V)$ curves traced in such experiments consisted of pronounced peaks indicating the sum-gap voltage V_g . The superconducting gap $2\Delta = V_g/N$ was deduced to be 50 meV at 10 K and to show a nearly BCS-like temperature dependence. A PG was also observed to evolve below 150 K, where the c -axis resistivity ρ_c becomes increasing on decreasing temperature [77], see figure 10. Of

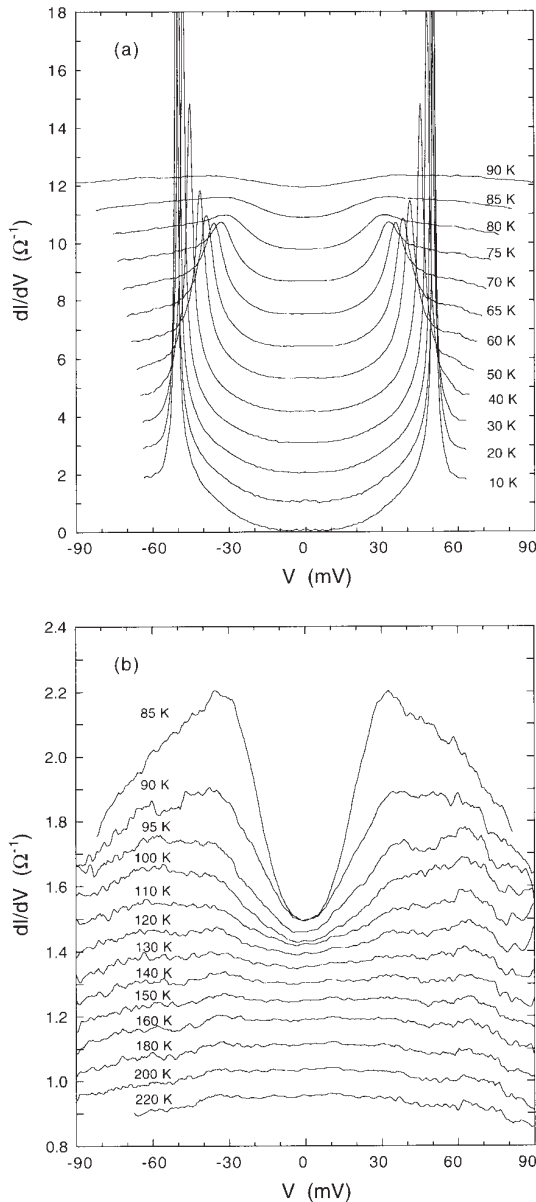


Figure 10. (a) $dI/dV-V$ curves below T_c obtained numerically from the data. Each curve is shifted by $1 \Omega^{-1}$ to make it easier to see. (b) $dI/dV-V$ curves above T_c . Each curve is shifted by $0.05 \Omega^{-1}$. (From M Suzuki, T Watanabe and A Matsuda 1999 *Phys. Rev. Lett.* **82** 5361, [77]; ©1999 The American Physical Society.)

importance here are the facts that (i) the PG is present in overdoped Bi-2212, which confirms earlier STM studies on Bi-2212 samples [84], and (ii) the PG is not due to trivial overheating. The superconducting gap feature below T_c looked to gradually pass into the pseudogap with temperature increasing through T_c without a noticeable peculiarity at $T = T_c$. Such a transformation may give rise to speculations on pre-formed pairs above T_c , and on considering PG as a precursor of superconductivity [84]. Suzuki *et al* avoid, however, drawing such a conclusion from their experiments [76]. See, however, their very recent work, [78], where this conclusion has been actually made, being based on experiments involving mesas with different oxygen content.

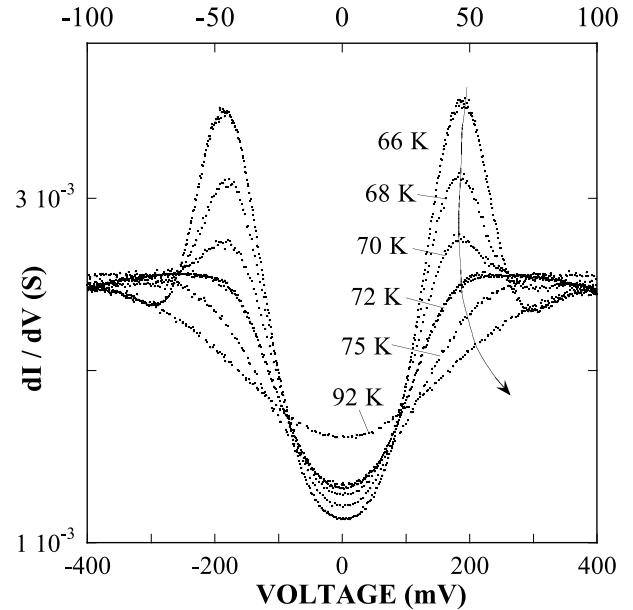


Figure 11. The c -axis intrinsic tunnelling spectra for HgBr_2 -Bi2212 single crystal at different temperatures close to $T_c \approx 70 \text{ K}$. The number of intrinsic junctions $N = 4$. The arrow indicates the approximate position of the $dI/dV(V)$ maxima (which would represent the superconducting gap at low temperatures). Upper scale corresponds to V/N .

In a set of experiments on mesa structures patterned on surfaces of Bi-2212 single crystals [81] and the same crystals intercalated with HgBr_2 [83], the authors clearly observed that the PG and superconducting gap coexist below T_c . The intercalation turned out to be an effective way for reducing j_c and hence internal overheating, leaving T_c almost unchanged. Note that the tunnelling barriers in intrinsic Josephson junctions of intercalated Bi-2212 are of a very high quality. Re-scaling the resistance of individual IJJ down to the area s typical for STM measurements (say, $\sim 5 \times 5 \text{ \AA}^2$), resistances as high as $10^{12} \Omega$ can be obtained. Such values are even larger than the resistances of tip-to-surface tunnel barriers in STM experiments.

PG exists at all temperatures making a sort of ‘background’ for other features of tunnelling spectra, superconducting peaks and dips at $V \approx 3\Delta(T)$ [85]. The superconducting gap peaks move towards zero with increasing T , gradually losing their distinctiveness on approaching T_c . This is similar to the STM measurements [84], see figure 11, and may be reminiscent of having PG and superconducting gaps merging at $T \lesssim T_c$. The loss of distinctiveness does not allow the precise location of the superconducting gap position. However, branches of the $I-V$ characteristics at a small current are still distinct even close to T_c (typically, up to $T \approx T_c - 1$). Assuming that the voltage jumps δV between branches are proportional to the superconducting gap, from the fact that $\delta V_{I=\text{const}} \rightarrow 0$ at $T \rightarrow T_c$, it was attested that the superconductivity does quench at T_c [81].

The shapes of $R_c(T)$ dependences of both the pristine Bi-2212 and HgBr_2 -Bi2212 look very much alike, see figure 12, despite a 20-fold difference in the absolute values. This means that the coupling between CuO_2 bilayers has no effect

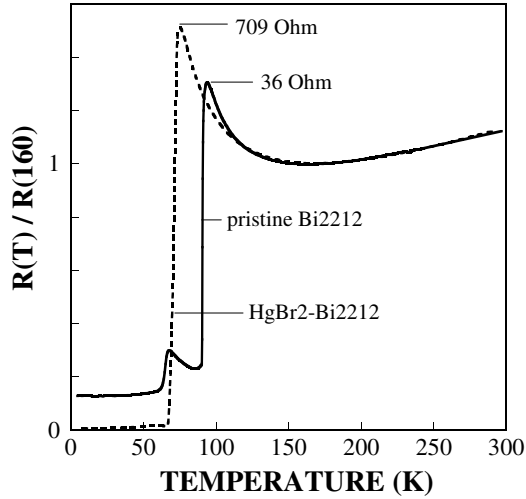


Figure 12. The $R_c(T)$ curves normalized by $R_c(160)$ for both pristine and intercalated samples. The numbers of junctions in these two samples are nearly the same ($N = 12\text{--}14$). Note the 20-fold difference in absolute values of resistance at $T \gtrsim T_c$. The second ‘transition’ for the pristine Bi-2212 sample is due to 1–2 deteriorated junctions [25, 68] underneath the contact to the stack in the three-probe measurements.

on the shape of the c -axis resistivity. The semiconductor-like $R_c(T)$ seems to be fully governed by the properties of individual CuO_2 bilayers. This throws discredit upon several models, like the thermally activated hopping model [86], and, perhaps, the resonant tunnelling model [87] of the c -axis transport, because the intercalation most likely changes both the hopping probability and number of resonant centres.

6.3. Vortex matter

The physics of vortices appears to play a large part in high-temperature superconductivity. High transition temperatures, a layered structure and a short coherence length are the most unique properties of the new superconductors. Thermal fluctuations, which are particularly large in HTS, set the region of the B – T phase diagram where the vortex lattice can melt into a liquid. Different melting scenarios have been the topic of intense discussion during recent years.

The vortex lines in highly anisotropic layered HTS materials like Bi-2212 consist of the so-called pancake vortices. The superconducting screening currents of the individual vortices are confined to CuO_2 planes. Between the planes, there is only a weak Josephson coupling (plus magnetic interaction) which makes the fragments of an individual vortex line stack on top of each other. The disorder in the system, like the oxygen or crystal structural defects can impose irregular pinning potential on the vortex system. It may then be more favourable for the pancake to break the straightness of the vortex line and jump to a nearby pinning centre. This ‘wandering’ of pancakes causes the appearance of the in-plane component of the magnetic field, or the Josephson ‘string’. In its turn, the local in-plane magnetic field produces the local phase variance. Being averaged over the space and time, it leads to a decrease of j_c [88].

Measurements of j_c in the magnetic field can therefore provide information on the out-of-plane correlation of the

pancakes. So far, the main experimental method of studying this was the Josephson plasma resonance (JPR). There are several features of the B – T phase diagram as seen in such experiments, involving the melting of the vortex lattice and some peculiar lines in the liquid phase of the vortex system. Assuming a sinusoidal phase relation, the critical current can be related to the microwave plasma resonance [89, 90]. j_c is then proportional to the square of the frequency of Josephson oscillations, $j_c \propto \omega_p^2$ [91]. It has also been shown that both j_c and ω_p are equivalent in giving information about the interlayer phase coherence [92].

6.3.1. Intrinsic Josephson junctions in a perpendicular magnetic field.

IJJ in a perpendicular magnetic field have been studied relatively little. The majority of published measurements of the c -axis electrical characteristics in the magnetic field have been made using single crystals, in which the Josephson nature of the interlayer coupling has simply been assumed, without any direct justification.

A detailed study of IJJ in a perpendicular magnetic field B_\perp with direct measurements of the c -axis current–voltage characteristics has been performed recently [93, 94]. The multi-branched I – V characteristics pointed to the intrinsic Josephson effect in the samples with different oxygen content. Oxygen content had a pronounced effect on j_c in the zero magnetic field— j_c was four times larger in the oxygenated samples. In a non-zero B_\perp , the c -axis resistance R_c develops a peak below the zero-field superconducting transition temperature T_{c0} . The magnitude of this magneto-resistance peak effect (MRPE) appeared to be inversely proportional to j_c or the oxygen content. In principle, the MRPE can be predicted from just zero-field measurements, as it comes from a competition between the sub-gap resistance R_{sg} of IJJ at $V \rightarrow 0$ and the Josephson coupling. The former can be directly deduced from the I – V characteristics. The one-to-one correlation between the zero-field R_{sg} and the R_c in the mixed state of Bi-2212 has been experimentally demonstrated in [95].

Figure 13 shows $I_c(T, B_\perp)$ for the oxygen annealed sample in magnetic fields of 0, 0.4, 1 and 2 T parallel to the c -direction. All measurements were made on warming in a constant field, applied before first cooling from above T_c , to ensure as uniform a distribution of flux across the mesa as possible. Generally, the critical current I_c decreases with applied field over the whole temperature range. On warming in a finite field, I_c increases to a peak in the temperature range 15 to 25 K. At low temperatures the variation in I_c from measurement to measurement increases as the temperature decreases, as illustrated by the increased size of the error bars. This is contrary to what would have been expected had thermal or extrinsic noise been the dominant source of the variation. The fluctuations in critical current could be explained either by stochastic fluctuations in the pinned vortex state from one cycle to the next, or by different metastable configurations of Josephson vortices trapped between the planes [96].

Above the peak at $T \approx \tilde{T}$, the critical current decreases, but with no onset of any resistance at low current bias. However, at $T_{irr}(B_\perp)$, which is identified as the irreversibility

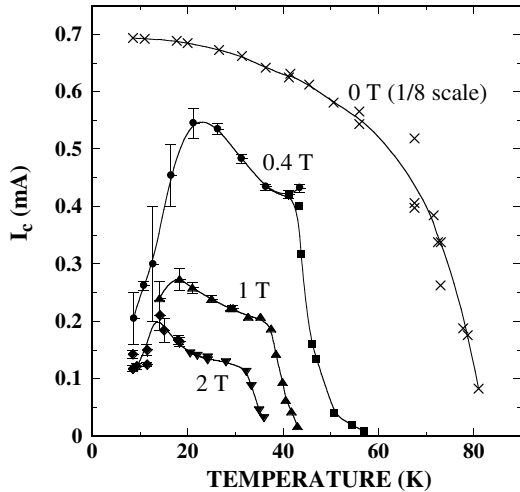


Figure 13. Temperature dependence of the c -axis critical current for perpendicular magnetic fields as indicated. Symbols correspond to the critical current I_c defined using a 0.1 mV voltage criterion or from the critical current distribution functions $P(I_c)$. The lines drawn through the experimental points are only intended as guides for the eye [93].

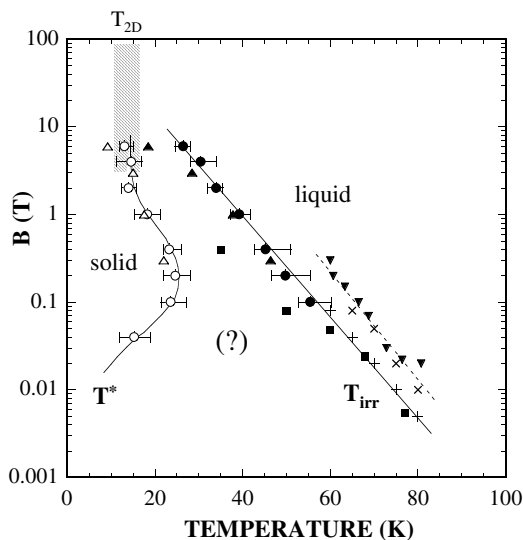


Figure 14. B - T diagram of vortex phases for fields perpendicular to the ab -planes suggested from the measurements of [93]. Open symbols represent the field dependence of the temperature \tilde{T} at which the maximum $I_c(B_\perp, T)$ dependence is observed. The irreversibility line was inferred from different measurements on Bi-2212 single crystals, see [93].

temperature, the characteristics become resistive at small voltages.

\tilde{T} and T_{irr} define three regions of the B - T phase diagram, see figure 14. This involves two solid phases below T_{irr} , where a zero voltage is observed, and a liquid phase above T_{irr} , where the c -axis conduction is dissipative.

Irradiation by high-energy heavy ions, which produce columnar defects (CD)s across the whole thickness of a single crystal is believed to improve the c -axis correlation of the pancakes, and is expected to increase both the in-plane and out-of-plane critical currents. A regular triangular-lattice arrangement of CD)s would lead to features in the c -axis

correlation of pancakes at the matching field B_ϕ (when the number of vortices equals the number of CD)s and its integer fractions [97]. For a more realistic situation of randomly distributed CD)s it was numerically shown that the trapping rate of the pancakes as a function of the magnetic field B has a feature at $B = 1/3 B_\phi$ [98]. The I_c of Bi-2212 mesas with columnar defects does indeed show a pronounced maximum at $\approx B_\phi$ and shows no feature at $B = B_\phi$ [99].

6.3.2. Intrinsic Josephson junctions in a parallel magnetic field. IJJ in a parallel magnetic field B_\parallel have been studied more intensively due to potential applications for Josephson transmission lines or vortex-flow three-terminal devices. Theoretically, the system of stacked Josephson junctions is described by the coupled sine-Gordon equation, usually using the formalism of Sakai *et al* [100] and numerical simulations. The analytic solution for static and dynamic properties of stacked Josephson junctions has also been worked out [96]. The developments in this area have already been reviewed by Pedersen and Ustinov [101].

Low-temperature $(\text{Nb-Al-Ox})_2\text{-Nb}$ stacked tunnel junctions may serve as pilot models for intrinsic Josephson stacks in Bi-2212, despite their low T_c and a possible difference in the nature of superconductivity and geometrical sizes of electrodes. Dynamic and static behaviour of the Josephson vortices in such low-temperature stacks of Josephson junctions is still a subject of intense experimental and theoretical investigations [102–106].

Intrinsic Josephson junctions have very thin superconducting electrodes, much thinner than the London penetration depth λ_{ab} . In a finite in-plane field, coupling via currents flowing along the superconducting layers become essential [107]. In all fields, the charging effects [108, 109] and the non-equilibrium quasi-particle injection were also anticipated as a coupling mechanism [110].

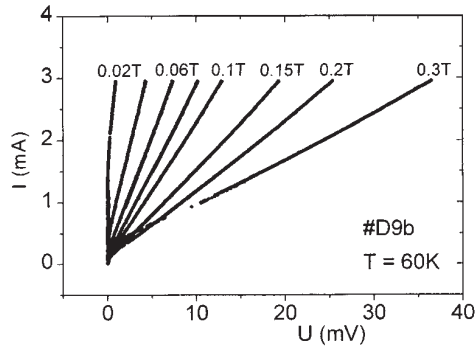
The structure of the supercurrent distribution around the Josephson vortex in an anisotropic high- T_c superconductor was calculated by Clem and Coffey [111]. The characteristic sizes of a Josephson vortex in such a superconductor have two length scales, λ_c (in the in-plane direction) and λ_{ab} (in the c -axis direction), both much larger than the thickness of the intrinsic Josephson junction. The streamlines of the supercurrent around the vortex centre are therefore zigzag-like due to the intervening insulating layers [111].

For a magnetic field parallel to the CuO_2 planes, the focus of most studies has been to look for the expected Fraunhofer-type field dependence of the c -axis critical current [5, 6, 27]. The typical lateral sizes of IJJ are of the order of 10 μm , and are larger than the Josephson penetration length:

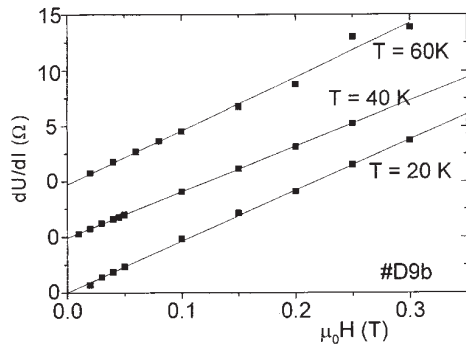
$$\lambda_J = \sqrt{\frac{\Phi_0 s}{2\pi \mu_0 \lambda_{ab}^2 j_c}}. \quad (3)$$

where Φ_0 is the unit flux, $s \approx 15 \text{ \AA}$ is the spacing between layers and μ_0 is the permeability of free space. $\lambda_J \sim 1 \mu\text{m}$ for typical $j_c \approx 10^3 \text{ A cm}^{-2}$ and $\lambda_{ab} \sim 2000 \text{ \AA}$. This means that in practically all experimental cases one meets complications due to formation of the Josephson vortices in $B_\parallel \neq 0$.

For SIS Josephson junctions with damping there is usually a resistive regime preceding the main critical current



(a)



(b)

Figure 15. (a) I - V characteristics of linear displaced branch for eight values of magnetic field. (b) Field dependence of linear slope $R = dU/dI$ for three different temperatures. (From G Hechtfischer *et al* 1997 *Phys. Rev. B* **55** 14 638, [115]; ©1997 The American Physical Society.)

transition to the first resistive branch, see figure 15. Such a behaviour was observed in linear stacks of artificial long Josephson junctions for fields parallel to the junction, and was identified with the vortex flow resistance [112, 113]. The vortex flow resistivity, defined as the dynamic resistance in the dissipative regime, is proportional to the magnetic field, see figure 15.

The vortex-flow behaviour in stacks of IJJ has been comprehensively studied in a number of experiments [23, 24, 43, 114, 115]. Vortex-flow resistivities ρ_{vf} of up to $10^{-3} \Omega \text{ cm G}^{-1}$ have been observed, which correspond to a voltage change of $\sim 0.03 \text{ mV G}^{-1}$ at a fixed bias current close to $I_c(B_{\parallel} = 0)$ [24]. The maximum velocity of Josephson vortices has been deduced from the experiments to be $\sim 3 \times 10^5 \text{ m s}^{-1}$ [114], which is very close to the theoretical value for the Swihart velocity $c_S = c_0 d / \lambda_{ab} \sqrt{\epsilon}$ [116], where $\epsilon \sim 25$ is the dielectric constant of the tunnelling barrier, and c_0 is the velocity of light. Irie *et al* obtained a factor of three higher velocity, $(1.5\text{--}1.8) \times 10^6 \text{ m s}^{-1}$, partly due to a smaller $\epsilon = 6$ used in their calculations [43].

A microwave emission in the vortex flow regime at various frequencies between 6 and 18 GHz was observed by Hechtfischer *et al* [115]. A broad resonance-like emission signal has been detected at voltages 0.5–1.5 mV, with higher voltages corresponding to higher receiver frequencies [115]. For the longest junctions (500 μm), the authors observed that

if they attached the bias and pick-up contact to one end of the stack, the microwave emission signal had an asymmetric form relative to the sign of bias current and applied magnetic field. The asymmetry corresponded to the direction of vortex motion; the larger emission occurred when vortices moved towards the microwave pick-up probe [115].

Comparatively little attention has been paid to the Josephson vortex state and its dynamics at *high* fields apart from the search for thermodynamic phase transitions [117, 118] and investigation of the angular dependence of the plasma frequency $\omega_p^2 \propto j_c(B)$ with field direction [119]. The field dependence of the critical current $I_c(B_{\parallel})$ determined from the major jump to the first resistive branch at $T = 25 \text{ K}$ was found to vary as $I_c \propto \exp(-B_{\parallel}/B_0)$, with $B_0 \approx 2.1$ and 2.5 T for the argon- and oxygen-annealed samples respectively [93]. This is consistent with earlier single crystal measurements by Latyshev *et al* [120].

The calculation of the density correlation function of the vortex liquid predicts approximately exponential decay of the c -axis critical current (plasma frequency) with the in-plane component of the magnetic field for fixed c -axis component [121]. The experiment may also be explained by assuming the small-bundle pinning regime of the Josephson vortices [93] for reasonable values of B_{\parallel} and experimentally unavoidable non-zero misorientation angle between the field and ab -planes.

In high parallel fields, $B > B_{cr} \sim 1.5 \text{ T}$, Hechtfischer *et al* observed a strong broad-band non-Josephson microwave emission which was not expected for conventional junctions. They explained the observation by Cherenkov radiation taking place when the vortex velocity exceeds the lowest velocity of electromagnetic wave in the stack [122]. See also the recent numerical simulations on locked superradiant vortex-flow states in stacks of IJJ [123].

6.4. Pressure experiments

The correlation between I_c of IJJ (as a direct measure of the interlayer coupling) and T_c (as a measure of the condensation energy) of the Bi-based compounds $\text{Bi}_2(\text{Sr}_{1.5}\text{La}_{0.5})\text{CuO}_{6+\delta}$ (Bi-2201) and Bi-2212 has been checked experimentally [124], using hydrostatic pressure $P \leq 1 \text{ GPa}$ as a tool to alter the interlayer coupling in the single crystals. All the experiments were done on one and the same single crystals, and the variation of parameters among different crystals was avoided.

It was observed that while the interlayer coupling (I_c) increases dramatically with pressure (up to 270 % GPa^{-1}), T_c only slightly increases at a rate of 2–6 % GPa^{-1} , see figure 16. These incommensurate effects of pressure suggest that the CuO interlayer coupling has little effect on T_c of the Bi compounds, in contrast to the ILT-model [124].

Important for understanding high-temperature superconductivity, these experiments can also provide a basis for technical solutions. For instance, one of the compounds from the Bi family, $(\text{Bi,Pb})_2\text{Sr}_2\text{Ca}_2\text{Cu}_3\text{O}_y$ (Bi-2223) has already found a utilization in the form of multi-filamentary tapes capable of carrying high currents without dissipation. The tapes are of interest for the development of superconducting motors, transformers and transmission lines. Critical current

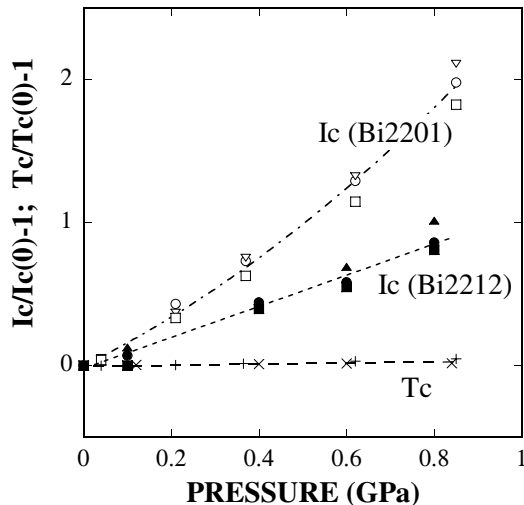


Figure 16. The relative changes of I_c (at different temperatures) and T_c with pressure for Bi-2212 and Bi-2201 [124].

densities j_c up to 70 kA cm^{-2} have been obtained in such tapes. Higher j_c values could be possible and optimization could move beyond the empirical approaches currently being used if a better understanding of the current limiting mechanisms were achieved.

It has been shown, for instance, that while j_c at low fields may be increased by improved processing which yields a better inter-grain connectivity, the high-field j_c can only be enhanced by strengthening the pinning of vortices within the Bi-2223 crystallites themselves [125]. In this respect, the 2–3-fold increase of the c -axis critical current under the pressure is promising for boosting the overall j_c of such tapes. One could possibly design the processing in such a way, that there are large residual stresses in the tape, which would most likely improve both the inter- and intra-grain connectivity of the tapes.

7. Possible applications of intrinsic Josephson junctions for three-terminal devices

Since the 1950s, when study of the superconducting three-terminal devices started with cryotrons [126], much attention has been paid to their development [127]. The interest in superconducting transistors is due to their potential advantages, like the ability to sustain high controllable current densities without energy dissipation. Moreover, superconducting transistors are compatible with other superconducting components, and may be required to interface with superconducting electronics. Research on the superconducting transistors has been intensified since the discovery of HTS, which opened ways of making relatively cheap devices operating at liquid nitrogen temperatures. There have already been made many attempts to fabricate different types of HTS transistors [128, 129]. The main types of superconducting transistors are: Josephson vortex-flow transistors, electric field-effect devices (SFETs), and quasiparticle-injection devices [128, 129]. They have been shown to work at liquid nitrogen temperatures and to have finite current or voltage gains.

Intrinsic Josephson junctions have an attractive feature, namely the SIS character of their $I-V$ characteristics, suitable for heterodyne (SIS) mixers. The wider energy gap of the high- T_c material may increase the operation of SIS mixers up to about 5 THz. Other interesting features are the extremely small thickness of the electrodes of each junction and the easiness of making stacks of different areas and heights. The latter is in a favourable contrast to all other types of high- T_c Josephson junctions, for which the fabrication of stacked planar structures has always been a problem. This makes this material promising for three-terminal devices, as will be explained below.

7.1. Quasiparticle-injection devices

The principle of such devices is the injection of non-equilibrium quasiparticles into the drain-source (DS) channel from the control electrode through a tunnel junction or weak link, formed on top of the DS channel. The interest in these devices arises from a potential current gain and a fast response time due to the creation of a non-equilibrium state. The characteristic relaxation time of such a state is of the order of 1–100 ps [128].

Figure 17(a) schematically shows the assumed arrangement of such a device with intrinsic Josephson junctions. The thickness of the electrodes which make the Josephson junctions in the Bi-2212 single crystals is extremely small, $\sim 3 \text{ \AA}$. This means that the injected high-energy quasiparticles can penetrate several unit cells deep into the Bi-2212 single crystal from its surface and influence the properties of many intrinsic Josephson junctions connected in series. This promises to increase the sensitivity and performance of a device involving many IJJ.

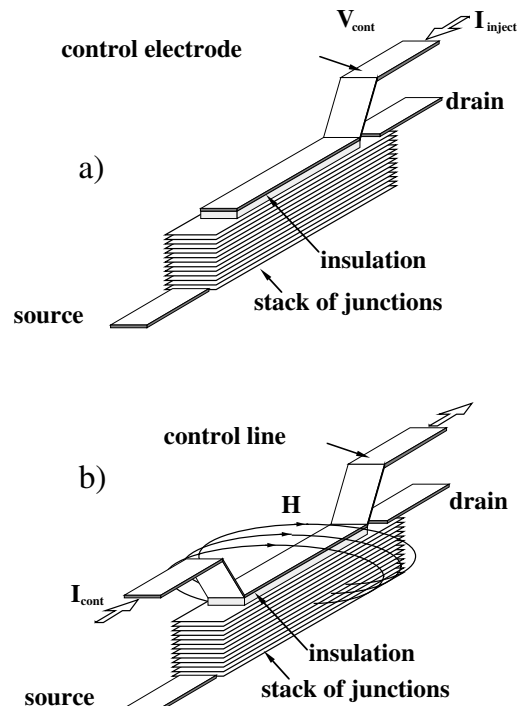


Figure 17. The suggested devices based on stacks of intrinsic Josephson junctions. (a) Quasiparticle-injection or field-effect transistors. (b) Vortex-flow transistor.

The change of the density of quasiparticles $\delta n = n - n_0(T)$ due to the current injection is:

$$\delta n = \frac{j \tau}{e d} \quad (4)$$

where j is the injection current density, τ is the effective recombination time, e is the electron charge, d is the quasiparticle penetration depth, n is the total density of quasiparticles, and $n_0(T)$ is the thermally excited density of quasiparticles. Taking $j \sim 10^3 \text{ A cm}^{-2}$, which corresponds to the injection current $I_{inj} \approx 1 \text{ mA}$ through $\sim 100 \mu\text{m}^2$ of the control electrode area, $d \sim 10\text{--}100 \text{ \AA}$, corresponding to the mean free path of quasiparticles, and $\tau \sim 1\text{--}100 \text{ ps}$, one gets $\delta n \sim 10^{10}\text{--}10^{11} \text{ cm}^{-3}$. This value has to be compared with $n_0(T)$. For a BCS superconductor, this number is exponentially decaying with decreasing temperature, $n_0(T) \propto \exp(-\Delta/T)$. To get $n_0(T)$ of the same order of magnitude as δn one has to work at low temperatures. Estimations show that the temperature should be less than 20–30 K for such a quasiparticle-injection device to work. The most indefinite parameter in this consideration is the effective recombination time τ and the mean free path of quasiparticles.

For quasiparticles injected at much higher than Δ energies this time involves the electron–phonon relaxation and phonon escape times due to an avalanche-like creation of the secondary quasiparticles. These times are usually several orders of magnitude longer than $\tau \sim 1\text{--}100 \text{ ps}$, used in the above estimation. This may drastically improve the low-frequency responsivity at $T \sim 70 \text{ K}$, but, unfortunately, decrease the cut-off frequency down to 1–10 GHz. One should therefore find a trade-off solution opting between speed and responsivity of the device.

7.2. Electric field-effect devices

An electric field applied to a superconductor via an insulating barrier changes the density of the Cooper pairs in a thin layer of the depth d of the superconductor close to the superconductor–insulator interface. As the pair potential of the superconductor is a function of the Cooper pair density, all superconducting properties in the field-penetrated layer depend on the applied electric field. The characteristic length, which has to be compared with the field-penetrated depth d is the superconducting coherence length ξ . The condition $d \geq \xi(T)$ should be satisfied for the effect of the applied field to be seen in the superconducting properties of the DS channel. In the majority of high- T_c superconductors, d is of the order of 1–10 nm [128, 130] and $\xi(T)$ is of the same order, in contrast to low- T_c ones, for which $d \ll \xi(T)$, and the field effects are small.

The arrangement of the suggested IJJ-FET transistor is the same as for the quasiparticle-injection one. The only difference is that the insulation layer between the control electrode and the stack should be made much thicker to have basically no input current between the two. This is promising for achieving a high current gain. Intrinsic Josephson junctions incorporated in such a type of device favourably feature in comparison to all other high- T_c junctions by their planar layered structure and their having a short coherence

length in the c -axis direction. As compared with the previous work [130], the suggested IJJ-FET is more feasible because all junctions affected by the electric field contribute to the output voltage, and even one IJJ is enough for the device to be operative.

Moreover, in the usual in-plane geometry [128, 130], the superconducting sheets which are further away from the gate electrode and which are less affected by the field, just short electrically the ‘useful’ ones. Therefore the field-response of thick layers of HTS material is basically much smaller than that for a thin layer $\sim 10 \text{ nm}$ [130].

7.3. Josephson vortex-flow transistors

In such devices, a drain-source (DS) channel is formed by a long Josephson junction or by a number of short Josephson junctions connected in parallel. The control line is usually put close to the channel, and the magnetic field induced by the current in the control line generates Josephson vortices in the junction. The vortices suppress the critical superconducting current I_c of the junction and, once they flow under the influence of the drain-source current I_{DS} , they change the junction resistance. Such transistors could have excellent decoupling of the input circuit from the output one and may operate at frequencies $\leq 500 \text{ GHz}$ [128].

A simplified schematic of the suggested device is shown in Figure 17(b). There is a stack of 10–100 intrinsic Josephson junctions with contacts on the top and near the base of the stack (drain and source). The dimensions of the stack, which can be used for estimations, are $100 \times 2 \times 0.05 \mu\text{m}^3$ (a ‘long’ junction). A thin-film control line on top of the stack is electrically isolated from the stack. The control current I_{cont} produces a magnetic field, which, once it becomes larger than the first critical field H_{c1} , generates the Josephson vortices in the stack. H_{c1} for the Bi-2212 material may be estimated from the formula [4]

$$H_{c1} = 4\pi \frac{e_J}{\Phi_0} \quad (5)$$

$$e_J \approx \gamma \gamma_0 \ln \frac{\lambda}{s} \quad (6)$$

where e_J is the line energy of the vortex, $\lambda \sim 150\text{--}200 \text{ nm}$ is the London penetration depth, γ is the anisotropy ratio (0.02–0.01 for the Bi-2212 compound) and $\gamma_0 = (\Phi_0/4\pi\lambda)^2$ is the characteristic energy scale, which determines the self-energy of the vortex. The estimation yields $H_{c1} \sim 10 \text{ G}$, which agrees with experiments on vortex flow in long stacks of IJJ [23, 24].

I_{cont} needed to induce such a magnetic field in the stack may be easily estimated from the formula $4\pi I_{cont}/cw$ for the magnetic field H_{\parallel} between the film and the superconducting ‘mirror’. Here c is the velocity of light and w is the width of the control line. For $w \sim 2 \mu\text{m}$, we get $I_{cont} \sim 1 \text{ mA}$. This means that just small currents are sufficient to control the vortex motion in the stack for the simplest geometry of the device.

7.4. High-frequency mixers and the voltage standard

The high critical temperature and superconducting gap, and the natural arrangement of stacked IJJ was thought to be

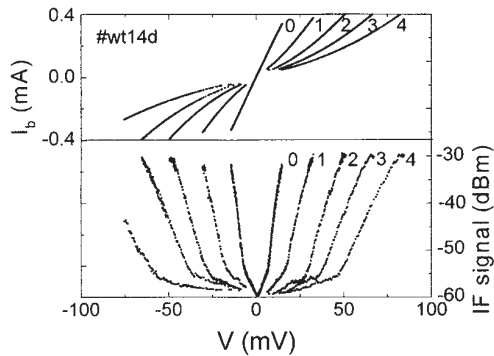


Figure 18. I - V characteristic (upper part) and intermediate-frequency (IF) intensity at 4.2 K and zero magnetic field (lower part). Constant resistance is not subtracted. The additional voltage drop is due to two-point measurement. The indices denote the number of junctions in the resistive state. (From W Walkenhorst *et al* 1997 *Phys. Rev. B* **56** 8396, [131]; ©1997 The American Physical Society.)

promising for (heterodyne) mixing to produce a conversion gain. If anything, the only successful attempt to use IJJ for mixing high-frequency signals so far has been undertaken in [131]. The observed W -band-mixing behaviour, see figure 18, could be explained by interactions between the external microwave signals and the collective Josephson plasma resonance of the stack of IJJ [131]. However, the present technology requirements for heterodyne mixers are too demanding for IJJ to be used at this time.

Another tempting application of the Josephson effect is the voltage standard based on hysteretic Shapiro steps crossing the voltage axis at zero current. While the LTS voltage standard has already been implemented in the form of large ($> 10\,000$) arrays of LTS junctions [132], HTS stacks of intrinsic junctions could be particularly attractive because of their high degree of portability and high operational temperature. The phase locking across the whole array can be easily achieved also because of the tiny thickness of intrinsic electrodes.

Microwave phase locking steps in stacks of IJJ have been successfully observed in the I - V curves of several studies [133–136]. The steps were sometimes composed of fundamental and several subharmonic ones [133, 134]. However, the effects were associated with vortex motion in the mesas of relatively large size rather than with the Shapiro zero-current-crossing voltage steps [133, 134, 135, 136]. Microwave experiments on small sub-micrometre-sized stacks are therefore advisable to avoid complications related to vortex motion.

8. Conclusions

Numerous experiments on the intrinsic Josephson effect have been conducted up to date. The literature on the subject is quite extensive. The experiments on IJE have already yielded many fresh insights into physics and our understanding of high-temperature superconductivity. The continuing research may hopefully lead to devices having useful technical applications as well.

Acknowledgments

I am grateful to Professors T Claeson, D Winkler, P Müller and R Kleiner for their interest and stimulating discussions. Financial support from the Swedish Superconductivity Consortium, TFR, the Royal Swedish Academy of Sciences, and, in part, from RFBR (grant 980217485a) is greatly appreciated.

References

- [1] Anderson P W 1997 *The Theory of Superconductivity in the High- T_c Cuprate Superconductors* (Princeton, NJ: Princeton University Press)
- [2] Cooper S L and Gray K E 1994 *Physical Properties of High Temperature Superconductors* vol 4, ed D M Ginsberg (Singapore: World Scientific) p 61
- [3] Zeldov E, Majer D, Konczykowski M, Geshkenbein V B, Vinokur V M and Shtrikman H 1995 *Nature* **375** 373
- [4] Blatter G, Feigel'man M V, Geshkenbein V B, Larkin A I and Vinokur V M 1994 *Rev. Mod. Phys.* **66** 1125
- [5] Kleiner R, Steinmeyer F, Kunkel G and Müller P 1992 *Phys. Rev. Lett.* **68** 2394
- [6] Kleiner R and Müller P 1994 *Phys. Rev. B* **49** 1327
- [7] Müller P 1995 *Adv. Solid State Phys.* **34** 1
- [8] Kleiner R and Müller P 1996 *Advances in Superconductivity* ed R Pinto, S K Malik, A K Grover and P Ayyub (New Delhi: New Age) p 172
- [9] Tachiki M and Yamashita T (ed) 1997 *Proc. 1st RIEC Int. Symp. on Intrinsic Josephson Effects and THz Plasma Oscillations in High- T_c Superconductors (1997, Sendai, Japan)*, *Physica C* **293** 1–306
- [10] Fang Y and Routbort J L 1994 *J. Appl. Phys.* **75** 210
- [11] Régi F X, Schneck J, Palmier J F and Savary H 1994 *J. Appl. Phys.* **76** 4426
- [12] Yurgens A, Winkler D, Zhang Y M, Zavaritsky N and Claeson T 1994 *Physica C* **235–240** 3269
- [13] Yurgens A, Winkler D, Zavaritsky N V and Claeson T 1997 *Appl. Phys. Lett.* **70** 1760
- [14] Irie A, Hirai Y and Oya G 1998 *Appl. Phys. Lett.* **72** 2159
- [15] Suzuki M, Tanabe K, Karimoto S and Hidaka Y 1997 *IEEE Trans. Appl. Supercond.* **7** 2956
- [16] Itoh M, Karimoto S, Namekawa K and Suzuki M 1997 *Phys. Rev. B* **55** R12001
- [17] Suzuki M, Hidaka Y, Tanabe K, Karimoto S and Namekawa K 1996 *Japan. J. Appl. Phys.* **35** L762
- [18] Suzuki M and Tanabe K 1996 *Japan. J. Appl. Phys.* **35** L482
- [19] Odagawa A, Sakai M, Adachi H, Setsune K, Hirano T and Yoshida K 1997 *Japan. J. Appl. Phys.* **36** L21
- [20] Schmidl F, Pfuch A, Schneidewind H, Heinz E, Dörner L, Matthes A, Seidel P, Hübner U, Veith M and Steinbeiß E 1995 *Supercond. Sci. Technol.* **8** 740
- [21] Seidel P, Schmidl F, Pfuch A, Schneidewind H and Heinz E 1996 *Supercond. Sci. Technol.* **9** A9
- [22] Sakai M, Odagawa A, Adachi H and Setsune K 1998 *Physica C* **299** 31
- [23] Lee J U, Nordman J E and Hohenwarter G 1995 *Appl. Phys. Lett.* **67** 1471
- [24] Lee J U, Gray K, Nordman J E, Guptasarma P and Hinks D 1997 *Physica C* **293** 118
- [25] Kim N, Doh Y-J, Chang H-S and Lee H-J 1999 *Phys. Rev. B* **59** 14639
- [26] Yurgens A, Winkler D, Zavaritsky N V and Claeson T 1996 *Phys. Rev. B* **53** R8887
- [27] Latyshev Y I, Nevelskaya J E and Monceau P 1996 *Phys. Rev. Lett.* **77** 932
- [28] Latyshev Y I, Monceau P and Pavlenko V N 1997 *Physica C* **293** 174
- [29] Latyshev Y I, Gorlova I G, Nikitina A M, Antokhina V U, Zubtsev S G and Kukhta N P 1993 *Physica C* **216** 471

- [30] Latyshev Y I, Kim S-J and Yamashita T 1999 *JETP Lett.* **69** 84
- [31] Latyshev Y I, Yamashita T, Bulaevskii L N, Graf M J, Balatsky A V and Maley M P 1999 *Phys. Rev. Lett.* **82** 5345
- [32] Tsai J S, Fujita J and Kupriyanov M Y 1995 *Phys. Rev. B* **51** 16267
- [33] Yan S I, Fang L, Si M S and Wang J 1997 *J. Appl. Phys.* **82** 480
- [34] Ishibashi T, Sato K, Lee K and Iguchi I 1997 *Proc. 3rd Eur. Conf. on Applied Superconductivity, EUCAS'97 (Inst. Phys. Conf. Ser. 158)* vol 1 (Bristol: Institute of Physics) p 527
- [35] Veith M, Eick T, Kohler T, Brodtkorb W, Steinbeiß E, Schlenga K, Hechtfisher G and Müller P 1995 *Proc. 2nd Eur. Conf. on Applied Superconductivity, EUCAS'95 (Inst. Phys. Conf. Ser. 148)* vol 2 (Bristol: Institute of Physics) p 1435
- [36] Ishimaru Y, Wen J, Utagawa T, Koshizuka N and Enomoto Y 1997 *Physica C* **293** 196
- [37] Nakajima K, Sudo S, Tachiki T and Yamashita T 2000 *Proc. 4th Eur. Conf. on Applied Superconductivity (Sitges, Spain, 1999) (Inst. Phys. Conf. Ser. 167)* (Bristol: Institute of Physics) to be published
- [38] Bozovic I and Eckstein J N 1996 *Physical Properties of High Temperature Superconductors* vol 5, ed D M Ginsberg (Singapore: World Scientific) p 99
- [39] Renner Ch and Fisher Ø 1995 *Phys. Rev. B* **51** 9208
- [40] Miyakawa N, Guptasarma P, Zasadzinski J F, Hinks D G and Gray K E 1998 *Phys. Rev. Lett.* **80** 157
- [41] Winkler D and Claeson T 1985 *Phys. Scr.* **32** 317
- [42] Yasuda T, Tonouchi M and Takano S 1997 *Physica C* **289** 109
- [43] Irie A, Hirai Y and Oya G 1998 *Appl. Phys. Lett.* **72** 2159
- [44] Tanabe K, Hidaka Y, Karimoto S and Suzuki M 1996 *Phys. Rev. B* **53** 9348
- [45] Schlenga K, Hechtfisher G, Kleiner R, Walkenhorst W, Müller P, Johnson H L, Veith M, Brodtkorb W and Steinbeiß E 1996 *Phys. Rev. Lett.* **76** 4943
- [46] Ma J, Quitmann C, Kelley R J, Berger H, Margaritondo G and Onellion M 1995 *Science* **267** 862
- [47] Buzdin A I, Damjanovic V P and Simonov A Y 1992 *Physica C* **194** 109
- [48] Abrikosov A A 1997 *Phys. Rev. B* **55** 11735
- [49] Halbritter J 1994 *Proc. Workshop on HTS Josephson Junctions and 3-Terminal Devices (University of Twente, The Netherlands)* p 30
- [50] Johansson G, Shumeiko V S, Bratus E N and Wendin G 1997 *Physica C* **293** 77
- [51] Kresin V Z, Wolf S A and Ovchinnikov Y N 1996 *Phys. Rev. B* **53** 11831
- [52] Solimar L 1972 *Superconducting Tunneling & Applications* (London: Chapman & Hall)
- [53] Uematsu Y, Nakajima K, Yamashita T, Tanaka I and Kojima H 1998 *Appl. Phys. Lett.* **73** 2820
- [54] Rapp M, Murk A, Semerad R and Prusseit W 1996 *Phys. Rev. Lett.* **77** 928
- [55] Wang H B, Chen J, Tachiki T, Mizugaki Y, Nakajima K and Yamashita T 1999 *J. Appl. Phys.* **85** 3740
- [56] Uher C 1992, in *Physical Properties of High Temperature Superconductors* vol 3, ed D M Ginsberg (Singapore: World Scientific) p 159
- [57] Schlenga K, Kleiner R, Hechtfisher G, Mößle M, Schmitt S, Müller P, Helm Ch, Preis Ch, Forsthofer F, Keller J, Johnson H L, Veith M and Steinbeiß E 1998 *Phys. Rev. B* **57** 14518
- [58] Thomas P J, Fenton J C, Yang G and Gough C E 2000 *Preprint cond-mat/0001365*
- [59] Thomas P J, Fenton J C, Yang G and Gough C E 2000 *Physica B* **280** 245
- [60] Suzuki M, Watanabe T and Matsuda A *IEEE Trans. Appl. Supercond.* **9** 4507
- [61] Stupp S E, Lee W C, Giapintzakis J and Ginsberg D M 1992 *Phys. Rev. B* **45** 3093
- [62] Kim N, Chang H-S, Lee H-J and Doh Y-J 2000 *Preprint cond-mat/0003330*
- [63] Wolf E L 1989 *Principles of Electron Tunneling Spectroscopy* (Oxford: Oxford University Press)
- [64] Ekino T and Akimitsu J 1992 in *Studies of High Temperature Superconductor* vol 9, ed A Narlikar (New York: Nova Science) p 259
- [65] Hasegawa T, Ikuta H and Kitazawa K 1992 *Physical Properties of High Temperature Superconductors* vol 3 ed D M Ginsberg (Singapore: World Scientific) p 623
- [66] *Studies of High Temperature Superconductor* vol 20, ed A Narlikar (New York: Nova Science)
- [67] Yurgens A, Litvinchuk A P, Mros N, Winkler D, Zavaritsky N V and Claeson T 1995 unpublished
- [68] Yurgens A, Winkler D, Zavaritsky N and Claeson T 1996 *Proc. of Oxide Superconductors: Physics and Nanoengineering II (Proc. SPIE 2697)* (Bellingham, WA: SPIE) p 433
- [69] Helm Ch, Preis Ch, Forsthofer F, Keller J, Schlenga K, Kleiner R and Müller P 1997 *Phys. Rev. Lett.* **79** 737
- [70] See the comparison with experiments and corresponding references in Helm Ch, Preis Ch, Walter Ch and Keller J 1999 *Preprint cond-mat/9909318*
- [71] Maksimov E G, Arseyev P I and Maslova N S 1999 *Solid State Commun.* **111** 391
- [72] Ponomarev Y G, Tsokur E B, Sudakova M V, Tchesnokov S N, Shabalin M E, Lorenz M A, Hein M A, Müller G, Piel H and Aminov B A 1999 *Solid State Commun.* **111** 513
- [73] Timusk T and Statt B 1999 *Rep. Prog. Phys.* **62** 61
- [74] Narlikar A (ed) 1999 *Studies of High Temperature Superconductor: Pseudogap in High Temperature Superconductors* vol 27, ed A Narlikar (New York: Nova Science)
- [75] Maly J, Jankó B and Levin K 1998 *Preprint cond-mat/9805018*
- [76] Suzuki M, Karimoto S and Namekawa K 1998 *J. Phys. Soc. Japan* **67** 732
- [77] Suzuki M, Watanabe T and Matsuda A 1999 *Phys. Rev. Lett.* **82** 5361
- [78] Suzuki M, Watanabe T, Matsuda A 2000 *Preprint*
- [79] Luo S, Yang G and Gough C E 1995 *Phys. Rev. B* **51** 6655
- [80] Parker I F G, Gough C E, Endres M, Thomas P J, Yang G and Yurgens A 1998 in *Proc. of Conf. on Superlattices II: Native and Artificial (Proc. SPIE 3480)* (Bellingham, WA: SPIE) p 11
- Parker I F G, Endres M, Thomas P J, Yang G, Yurgens A and Gough C E 1998 *Preprint cond-mat/9809328*
- [81] Krasnov V M, Yurgens A, Winkler D, Delsing P and Claeson T 2000 *Phys. Rev. Lett.* **84** 5860
- [82] Müller P, Rother S, Waldmann O, Heim S, Mößle and Kleiner R 2000 *Preprint*
- [83] Yurgens A, Winkler D, Claeson T, Hwang S-J and Choy J-H 1999 *Int. J. Mod. Phys. B* **13** (1999) 3758 see also *Preprint cond-mat/9907159*
- [84] Renner Ch, Revaz B, Genouf J-Y, Kadowaki K and Fisher Ø 1998 *Phys. Rev. Lett.* **80** 149
- [85] DeWilde Y, Miyakawa N, Guptasarma P, Iavarone M, Ozyuzer L, Zasadzinski J F, Romano P, Hinks D G, Kendziora C, Crabtree G W and Gray K E 1998 *Phys. Rev. Lett.* **80** 153
- [86] Crommie M F and Zettl A 1991 *Phys. Rev. B* **43** 408
- [87] Abrikosov A A 1999 *Physica C* **317-318** 154
- [88] Bulaevskii L N, Pokrovsky V L and Maley M P 1996 *Phys. Rev. Lett.* **76** 1719
- [89] Tsui O K C, Ong N P, Matsuda Y, Yan Y F and Peterson J B 1994 *Phys. Rev. Lett.* **73** 724
- [90] Matsuda Y, Gaifullin M B, Kumagai K, Kadowaki K and Mochiki T 1995 *Phys. Rev. Lett.* **75** 4512
- [91] Bulaevskii L N, Pokrovsky V L and Maley M P 1996 *Phys.*

- Rev. Lett.* **76** 1719
- [92] Yasuda T, Uchiyama T, Fukami T, Aomine T and Takano S 1997 *Proc. 6th Int. Superconductive Electronics Conf. (1997, Berlin)* vol 2 (Braunschweig: Physikalisch-Technische Bundesanstalt) p 141
Yasuda T, Uchiyama T, Fukami T, Aomine T and Takano S 1998 *Applied Supercond.* **6** 337
- [93] Yurgens A, Winkler D, Claeson T, Yang G, Parker I F G and Gough C E 1999 *Phys. Rev. B* **59** 7196
- [94] Gough C E, Thomas P J, Fenton J C and Yang G 2000 *Preprint cond-mat/0002246*
- [95] Yurgens A, Winkler D, Zavaritsky N V and Claeson T 1997 *Phys. Rev. Lett.* **79** 5122
- [96] Krasnov V M and Winkler D 1997 *Phys. Rev. B* **56** 9106
- [97] Moshchalkov V V, Baert M, Metlushko V V, Rosseel E, Bael M J V, Temst K, Bruynseraede Y and Jonckheere R 1998 *Phys. Rev. B* **57** 3615
- [98] Sugano R, Onogi T, Hirata K and Tachiki M 1998 *Phys. Rev. Lett.* **80** 2925
- [99] Yurgens A, Konczykowski M, Mros N, Winkler D and Claeson T 1999 *Phys. Rev. B* **60** in press
- [100] Sakai S, Bodin P and Pedersen N F 1993 *J. Appl. Phys.* **73** 2411
- [101] Pedersen N F and Ustinov A V 1995 *Supercond. Sci. Technol.* **8** 389
- [102] Ustinov A V, Malomed B A and Sakai S 1998 *Phys. Rev. B* **57** 11691
- [103] Sakai S, Ustinov A V, Thyssen N and Kohlstedt H 1998 *Phys. Rev. B* **58** 5777
- [104] Goldobin E, Kupriyanov M Y, Nevirkovets I P, Ustinov A V, Blamire M G and Evetts J E 1998 *Phys. Rev. B* **58** 15078
- [105] Thyssen N, Monaco R, Petraglia A, Costabile G, Kohlstedt H and Ustinov A V 1999 *Phys. Rev. B* **59** 181
- [106] Goldobin E and Ustinov A V 1999 *Phys. Rev. B* **59** 11532
- [107] Kleiner R, Müller P, Kohlstedt H, Pedersen N F and Sakai S 1994 *Phys. Rev. B* **50** 3942
- [108] Koyama T and Tachiki M 1996 *Phys. Rev. B* **54** 16183
- [109] Preis C, Helm C, Keller J, Sergeev A and Kleiner R 1998 *Proc. Superconducting Superlattices II: Native and Artificial (San Diego) (Proc. SPIE 3480)* (Bellingham, WA: SPIE) p 236
- [110] Sakai M, Odagawa A, Adachi H and Setsune K 1998 *Physica C* **299** 31
- [111] Clem J R and Coffey M W 1990 *Phys. Rev. B* **42** 6209
- [112] Scott A C and Johnson W E 1969 *Appl. Phys. Lett.* **14** 316
- [113] Pedersen N F 1986 *Solitons* ed S E Trullinger, V E Zakharov and V L Pokrovsky (Amsterdam: Elsevier) p 469
- [114] Lee J U and Nordman J E 1997 *Physica C* **277** 7
- [115] Hechtfischer G, Kleiner R, Schlenga K, Walkenhorst W, Müller P and Johnson H L 1997 *Phys. Rev. B* **55** 14638
- [116] Bulaevskii L N, Zamora M, Baeriswyl D, Beck H, Clem J M 1994 *Phys. Rev. B* **50** 12831
- [117] Zavaritsky V N 1996 *Phys. Scr. T* **66** 230
- [118] Fuhrer M S, Ino K, Oka K, Nishihara Y and Zettl A 1997 *Solid State Commun.* **101** 841
- [119] Bulaevskii L N, Maley M, Safar H and Domínguez D 1996 *Phys. Rev. B* **53** 6634
- [120] Latyshev Y I and Volkov A F 1991 *Physica C* **182** 47
- [121] Koshelev A E, Bulaevskii L N and Maley M P 1998 *Phys. Rev. Lett.* **81** 902
- [122] Hechtfischer G, Kleiner R, Ustinov A V and Müller P 1997 *Phys. Rev. Lett.* **79** 1365
- [123] Machida M, Koyama T, Tanaka A and Tachiki M 2000 *Physica C* **330** 85
- [124] Yurgens A, Winkler D, Claeson T, Murayama T and Ando Y 1999 *Phys. Rev. Lett.* **82** 3148
- [125] Dhallé M, Cuthbert M, Johnston M D, Everett J, R Flükiger, Dou S X, Goldacker W, Beales T P and Caplin A D 1997 *Supercond. Sci. Technol.* **10** 21
- [126] Buck D A 1956 *Proc. IRE* **44** 482
- [127] Bremer J W 1962 *Superconducting Devices (Electronic Science Series)* (New York: McGraw-Hill)
- [128] Mannhart J 1996 *Supercond. Sci. Technol.* **9** 49
- [129] Claeson T 1996 *Proc. Future Electron Devices Symp. (1996, Tokyo)*
- [130] Frey T, Mannhart J, Bednorz J G and Williams E J 1995 *Phys. Rev. B* **51** 3257
- [131] Walkenhorst W, Hechtfischer G, Schlötzer S, Kleiner R and Müller P 1997 *Phys. Rev. B* **56** 8396
- [132] Van Duzer T 1997 *IEEE Trans. Appl. Supercond.* **7** 98
- [133] Irie A, Iwama M and Oya G 1996 *Supercond. Sci. Technol.* **9** A14
- [134] Irie A and Oya G 1997 *Physica C* **293** 249
- [135] Latyshev Yu I, Monceau P and Pavlenko V N 1997 *Physica C* **293** 174
- [136] Prusseit W, Rapp M, Hirata K and Mochiku T 1997 *Physica C* **293** 25